Recent Advances in Imaging Around Corners

Tomohiro Maeda, Guy Satat, Tristan Swedish, Lagnojita Sinha, Ramesh Raskar
MIT Media Lab
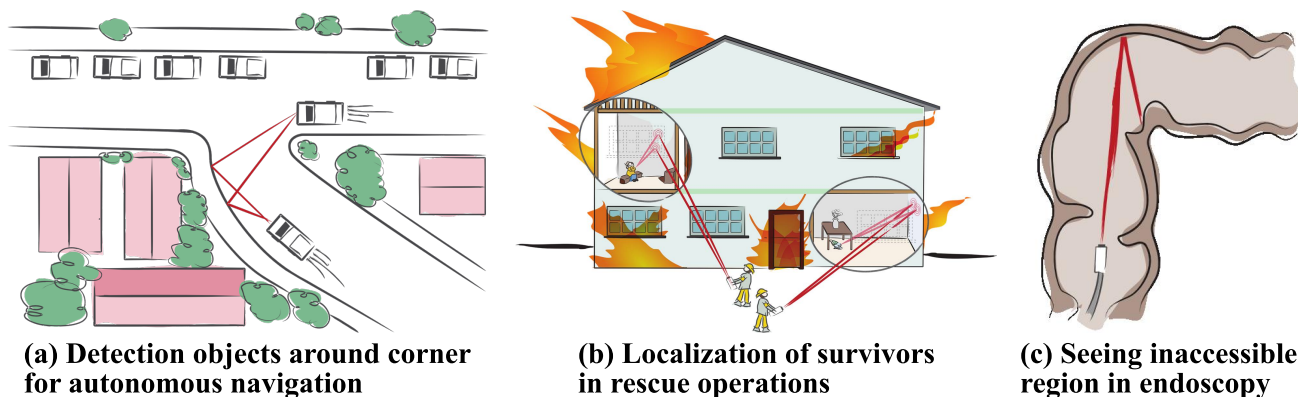
Figure 1: **Applications of non-line-of-sight (NLOS) imaging. (Material from:' [1], adapted with permission from the authors.')** (a) Detection of approaching vehicles around corners results in safer autonomous navigation. (b) Localizing survivors in the hidden areas makes search-and-rescue operations more efficient and safer. (c) Imaging the inaccessible regions in endoscopy enables better diagnostics.

Abstract

Seeing around corners, also known as non-line-of-sight (NLOS) imaging is a computational method to resolve or recover objects hidden around corners. Recent advances in imaging around corners have gained significant interest. This paper reviews different types of existing NLOS imaging techniques and discusses the challenges that need to be addressed, especially for their applications outside of a constrained laboratory environment. Our goal is to introduce this topic to broader research communities as well as provide insights that would lead to further developments in this research area.

1. Introduction

Recent advances in computational imaging techniques made it possible to image around corners, which is known as non-line-of-sight (NLOS) imaging. The ability to see around corners would be beneficial in various applications. For example, the detection of objects around a corner enables autonomous vehicles to avoid collisions. Detection and localization of people without the need to go into dangerous environments make rescue operations safer and more efficient. NLOS imaging can also be used for medical applications such as endoscopy, where the region of interest is hard for the sensors to access directly (Fig. 1).

Fig. 2 shows typical scene setups for NLOS imaging techniques. While there are many techniques using the electromagnetic (EM) spectrum or acoustic waves to image around corners and through walls [2–4], we focus on works that use light (electromagnetic wave in the visible and infrared spectrum). Fig. 3 shows an overview of the current state of NLOS imaging.

NLOS imaging was first proposed by Raskar and Davis [5], and demonstrated by Kirmani et al. [6] for recovery of hidden planar patches. Velten et al. [7] showed the first full reconstruction of a 3D object that was hidden around a corner. These works showed that ToF measurements of photons returning from the hidden scene with three bounces (Fig. 2 (a)) contain sufficient information to recover the occluded scene. Following these works, different sensing modalities were used for NLOS imaging. For example, Katz et al. [8] first demonstrated the use of a speckle pattern to reconstruct 2D images. Tancik et al. [9, 10] and Bouman
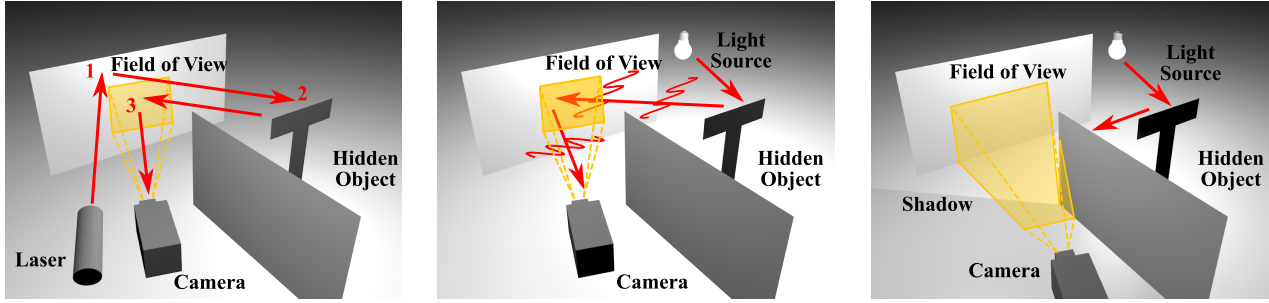
(a) Time-of-flight based methods exploit path-length constraints of photons

(b) Coherence-based methods exploit preserved coherence properties

(c) Intensity-based methods exploit shadows casted by depth discontinuities

Figure 2: **Layouts of typical NLOS imaging setups with different sensing principles.** (a) ToF-based techniques use three-bounce photons that give distance constraints. (b) Coherence-based techniques use speckle patterns or spatial coherence that are preserved during scattering. (c) Intensity-based methods mainly exploit occlusions that cast shadows.
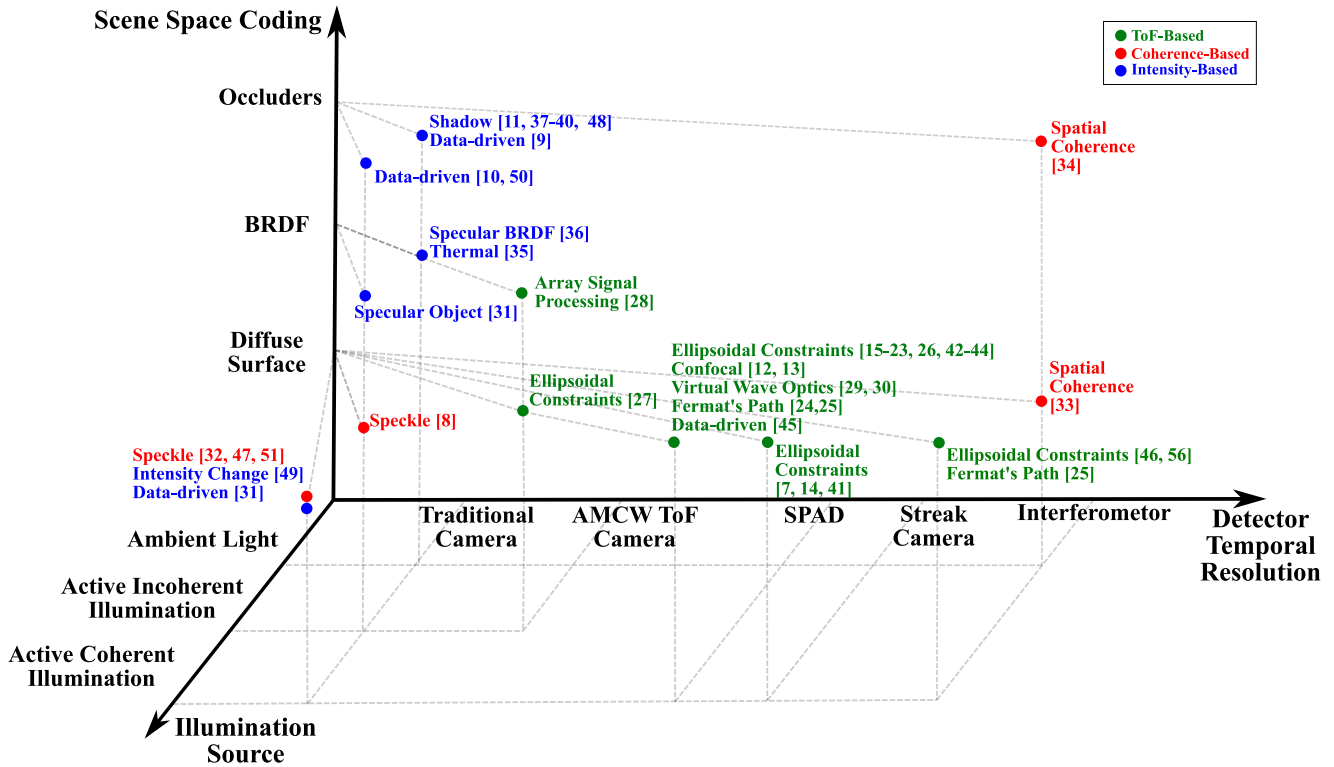

Figure 3: **Landscape of NLOS imaging works on detector, illumination source, and scene space coding.**

et al. [11] demonstrated reconstruction and tracking of the hidden object with a traditional RGB camera.

The main challenge in NLOS imaging is that the photons reflected from the hidden object are scattered at the line-of-sight surfaces (e.g., wall and floor). Computational imaging techniques model light transport to recover the information of the hidden scene. However, their applications in practice are still limited. This paper reviews the recent advances in NLOS imaging and discusses the challenges towards real-world applications. We note that other types of imaging tasks, such as seeing through scattering media, are often also referred to as NLOS imaging, but in this paper, we use the term "NLOS imaging" to refer solely to seeing around corners.

	ToF	Coherence	Intensity
3D Reconstruction	µm-cm Resolution [7, 12–30]	None	Planar/Specular Object [31]
2D Reconstruction	Included in 3D	Diffraction Limited Resolution [8, 32] cm Resolution [33, 34]	Coarse Resolution [31], Thermal [35] Occlusion Dependent [9, 10, 36–40]
Localization/ Tracking	cm Precision [41–46]	1D Distance Recovery [33] 3D Tracking [47]	Occlusion Dependent [10, 11, 48] 6D Tracking [49], 3D localization [35, 50]
Classification	Human Identification [45]	MNIST, Human Pose Classification [51]	Object Type Classification [10, 50], Human Pose Detection [35]

Table 1: **Overview of existing techniques to see around corners for different tasks.** The color of the table cell indicates the quality of the methods relative to other NLOS imaging techniques. Green and yellow cells indicate that NLOS imaging tasks have been shown in practical and limited recovery complexities. Red cells indicate that the tasks have not been demonstrated.

1.1. What is NLOS Imaging?

Fig. 2 illustrates different strategies to see around corners. Mathematically, NLOS imaging can be formulated as the following forward model:

$$\mathbf{y} = f(\mathbf{x}) + \epsilon, \qquad (1)$$

where, $\mathbf{x}$ represents the hidden scene parameters, such as albedo, motion or class of the hidden object, $\mathbf{y}$ is the measurement, $f(\cdot)$ is the mapping of the hidden scene to the measurement–which depends on the choice of illumination, sensor, and the geometry of the corner– and ϵ denotes the measurement noise.

The goal of NLOS imaging is to design sensing schemes such that $f(\cdot)$ can be inverted, and to build algorithms such that $\mathbf{x}$ is robustly and efficiently recovered given $\mathbf{y}$. Recently, data-driven approaches showed that inversion of Eq. 1 can be learned even when $f(\cdot)$ is not directly available [10].

Full Scene Reconstruction: The objective of NLOS imaging is to see around a corner as if there is a line-of-sight directly into the hidden scene. Reconstruction tasks include the recovery of the 3D, 2D, or 1D shape of the hidden object or light fields. In reconstruction, $\mathbf{x}$ is a direct representation of the hidden scene, such as a voxelized probability map, surface, or light transport in the hidden scene.

Direct Scene Inference: The reconstruction procedure often requires the long acquisition and time-consuming computations. However, full scene reconstruction might not even be necessary in many scenarios–for example, detecting the presence of a moving person is sufficient for rescue operations. We define "inference" as an estimation of these latent parameters

(e.g., location, class, or motion) without direct reconstruction of the hidden scene. In this case, the unknown parameter $\mathbf{x}$ can be location, type, or movement of the hidden object. Because inference does not require full reconstruction, inference around corners can be potentially performed with less computation and measurement than full scene reconstruction.

1.2. Overview of Sensing Schemes for NLOS Imaging

We classify the existing techniques into three categories based on their sensing modalities: Time-of-flight, coherence, and intensity. Table 1 provides an overview of the current state of each method regarding NLOS imaging tasks. Section 2–4 provides the review of NLOS imaging techniques that exploit different sensing modalities, and Section 5 presents the challenges of NLOS imaging for each category.

Time-of-Flight-Based Approach (Section 2): As the photons travel from the source, the first bounce occurs on an adjoining wall or directly on the floor near the corner. The second bounce is on the hidden object around the corner. The third bounce is again on a wall or a floor in the line-of-sight region and back towards the measurement system, as shown in Fig. 2 (a). Time-resolved imaging techniques utilize the photons associated with the third bounce, which constrains possible locations of the hidden object. Section 2 reviews the reconstruction and inference algorithms for time-resolved sensing based methods.

Coherence-Based Approach (Section 3): While the information on the hidden geometry is largely lost by the diffuse reflection of photons on the relay wall, some coherence properties of light are pre-

served. Coherence-based methods exploit the fact that coherence preserves information about the occluded scene. Section 3 reviews NLOS imaging techniques that utilize speckle and spatial coherence of light.

Intensity-Based Approach (Section 4): Occlusions from the corner or occlusions within the hidden scene can provide rich information on the hidden scene. Using occlusions, it is possible to recover the hidden scene with a typical intensity (RGB) camera, such as a smartphone camera (Fig. 2 (c)). While many intensity-based approaches rely on occlusions, some works demonstrate NLOS imaging by exploiting surface reflectance of the relay wall or the object. Section 4 reviews the intensity-based approach.

1.3. Cameras to Image Around Corners

Different hardware has been used to see around corners. We briefly introduce such hardware to describe what sensors and illumination sources are used for NLOS imaging.

Streak Camera + Pulsed Laser: A streak camera acquires temporal information by mapping the arrival time of photons in 1D space with sweep electrodes, resulting in a 2D measurement of space and time. Streak cameras offer the best time resolution down to sub-picosecond or even 100 femtoseconds (sub-mm –0.03 mm distance resolution), among other types of ToF cameras. The disadvantages of streak cameras are the high cost (typically more than $100k), low photon efficiency, high noise level, and the need for line scanning or additional optics [52]. This results in a potentially longer acquisition time for sufficient signal-to-noise ratio (SNR). The first works on NLOS imaging used a Hamamatsu C5680 for the experiments with Kerr lens mode-locked Ti:sapphire laser (50 fs pulse width).

SPAD + Pulsed Laser: Single-photon avalanche diode (SPAD) can detect the arrival of a single photon with a time jitter of 20–100 ps (6–30 mm distance resolution). Unlike streak cameras, it is possible to have 2D SPAD arrays for capturing 3D measurements without the need for line scanning. While the temporal resolution of a SPAD is poorer than streak cameras, the photon efficiency and SNR are better. Commonly used single-pixel SPAD detectors and time-correlated single-photon counting devices are from Micro Photon Devices and Hydraharp from PicoQuant. These cost around $5k and $20-35k, respectively.

AMCW ToF Camera + Modulated Light Source: An amplitude modulated continuous wave (AMCW) ToF camera compares the phase shift of emitted and received modulated light through three or more correlation measurements [53, 54]. The distance resolution of AMCW ToF cameras is limited by modulation frequency and the SNR. While AMCW ToF cameras can achieve few-mm resolution [55], they are susceptible to strong ambient light due to the need for a longer exposure time than that for pulse-based ToF cameras. AMCW ToF cameras have a much lower cost (ranging $400–$2000) than SPADs and streak cameras and are used in commercial products, including the Microsoft Kinect and Photonic Mixer Device (PMD).

Traditional Camera: In this paper, we use "traditional camera" to refer to the sensors such as charge-coupled device (CCD) and complementary metal-oxide-semiconductor (CMOS) arrays, which measure irradiance images without ToF information. Traditional cameras can be used for both intensity and speckle measurement modalities. The combination of a diffuser and traditional camera enables the measurement of cross-correlation of temporal coherence to provide passive ToF measurement [46]. Traditional cameras are the most ubiquitous and affordable sensor discussed in this paper but do not acquire direct measurements of time-of-flight information.

Interferometer: Interference between multiple lightwaves provides depth information in μm scale, which can be used for ToF-based NLOS imaging for microscopic scenes. For example, an optical coherence tomography system with temporally and spatially incoherent LED showed 10 μm resolution to demonstrate NLOS reconstruction of an object as small as a coin [25]. Heterodyne interferometry, which utilizes interference of light with different wavelengths, demonstrated NLOS imaging at 70 μm precision [56]. A dual-phase Sagnac interferometer captures complex-valued spatial coherence functions as a change of measured intensity and is used for spatial coherence-based methods. Such an interferometer is not commercially available, and we refer readers to [57] for the design and details of a dual-phase Sagnac interferometer. An interferometer is a sensitive instrument and often requires careful alignment and isolation from mechanical vibrations.

2. Time-of-Flight-Based NLOS Imaging

Among many numbers of works in NLOS imaging, ToF-based techniques are the most popular due to their ability to resolve the path length of the three-bounce photons that carry the information of the hidden scene. The ToF measurement of three-bounce photons can also be used for estimating the bidirectional reflectance distribution function (BRDF) of ma-
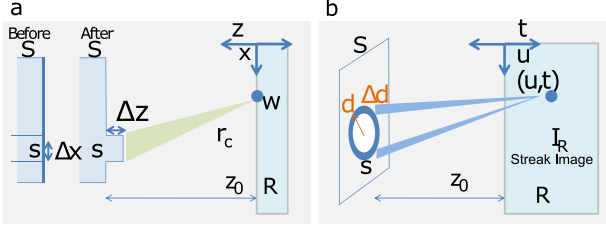
Figure 4: **Need for time-resolved information (Material from Velten et al., "Recovering three-dimensional shape around a corner using ultrafast time-of-flight imaging," published 2012, Nature Communications [7] with permission of the authors)**. a) Intensity change due to displacement of a patch is below traditional camera's sensitivity. (b) Temporal information resolves the displacement of a patch with a practical sensitivity range.

terials [58]. While this review paper only considers imaging around corners, ToF measurements are also useful for seeing through scattering media [59–63], analyzing light transport [64–71], and novel imaging systems [72–74].

The Benefit of ToF Measurement As discussed in the supplement material of Velten et al. [7], the change of intensity due to the displacement of a patch illustrated in Fig. 4 (a) is proportional to $(\Delta x)^2 \Delta z / z^3$, where Δ_x, Δ_z, z are the size, displacement and depth of a patch respectively. In contrast, the intensity change of a time-resolved measurement as illustrated in Fig. 4 (b) is proportional to $3\Delta x / (2\pi z)$. Drawing upon an example from [7], the fractional change of the intensity for $\Delta_x = 5$ mm, $\Delta_z = 5$mm, z = 20 cm is 0.00003 for the traditional camera and 0.01 for the ToF camera. This example shows that intensity change is below the sensitivity of the traditional camera. Furthermore, the SNR is small because the number of three-bounce photons is small. For this reason, the existing demonstration of intensity-based NLOS imaging relies on occlusions or more specular BRDF of the wall. ToF measurement can resolve the change of the measurement to recover the 3D geometry of the hidden object.

2.1. Reconstruction Algorithms

ToF measurements provide ellipsoidal constraints on the possible object locations in the hidden scene, as illustrated in Fig. 5. Let w_1 and w_2 denote points of the wall where a photon undergoes the first and third bounces, and o denote a point of the object where a photon undergoes the second bounce. Moreover, let l and v denote locations of the light source and the camera. Then the hidden object o must be on an ellipsoid
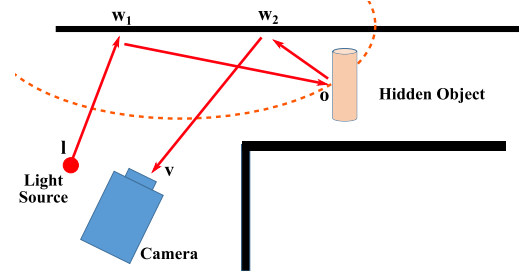

Figure 5: **Time-of-flight information gives constraints on the potential location of the object around corners.** When the path length of a photon is known, the location of the hidden object is constrained to the ellipsoid.
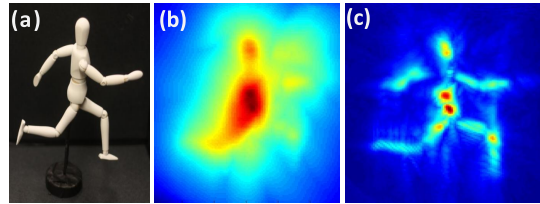

Figure 6: **Visualization of reconstruction via back-projection (Material from: Velten et al., "Recovering three-dimensional shape around a corner using ultrafast time-of-flight imaging," published 2012, Nature Communications [7] adapted with permission of SNCSC).** (a) The hidden object around the corner. (b) Probability map generated by a back-projection algorithm. (c) The contour of the object can be sharpened by applying a sharpening filter.

that satisfies

$$|w_1 - o| + |w_2 - o| = ct - |w_1 - l| - |w_2 - v|, \quad (2)$$

where c and t are the speed of light and time of travel respectively.

Most of the existing techniques consider discretized voxels to recover hidden geometry. This physics-based forward model maps the hidden scene to the measurement. Many works express the forward model with the ellipsoidal constraint as a linear inverse problem, which can be solved by back-projection or optimization.

$$\mathbf{y} = \mathbf{A}\mathbf{x} + \epsilon, \quad (3)$$

where $\mathbf{x} \in \mathbb{R}^n$ and $\mathbf{y} \in \mathbb{R}^m$ and $\epsilon \in \mathbb{R}^m$ denote the vectorized target voxels, ToF measurements, and noise respectively. $A \in \mathbb{R}^{m \times n}$ represents the transient light transport including the ellipsoidal constraints described by Eq. 2, intensity fall-off due to the surface reflectance, and the distance between the object and the
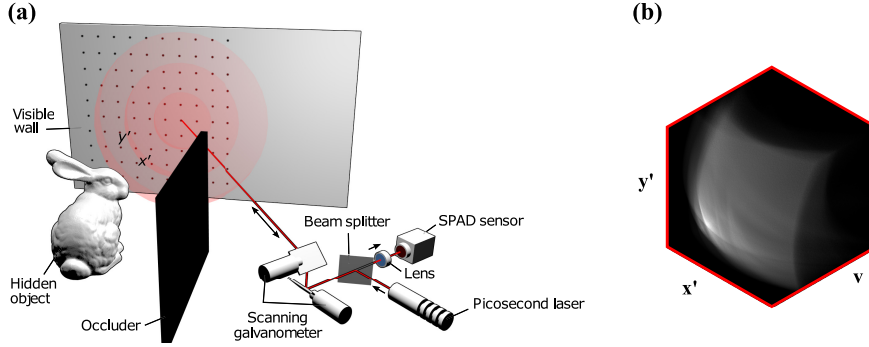
Figure 7: **Layout of Confocal imaging setup (Material from: O'Toole et al., "Confocal non-line-of-sight imaging based on the light-cone transform," published 2018, Nature [12], adapted with permission of SNCSC).** (a) The SPAD pixel and laser sees the same point on the wall. Due to the confocal optical design and change of variables, the measurement can be written as a convolution of the hidden object and a 3D kernel. (b) 3D kernel can be used to perform deconvolution to recover the hidden object.

wall. The theory of light transport of multi-bounce photons is studied by Seitz et al. [75] for non-time-resolved imaging, and by Raskar et al. [5] for time-resolved imaging.

In NLOS imaging, Eq. 3 is often ill-posed, so filtering or regularization of the reconstruction is often necessary. Moreover, $\mathbf{A}$ becomes large as x and y are 5D measurements (3D measurement $\times$ 2D scanning) and 3D voxels in general. For example, if we have $n_x \times n_y \times n_t$ 3D measurement for scanning illumination with n_s points, ith column of A_i has $n = n_x n_y n_t n_s$ elements, which maps the voxel x_i to the measurement. If we take $64 \times 64 \times \times 64$ 3D measurement with 64 laser illumination spots for $64 \times 64 \times 64$ voxel reconstruction, A is a 64^4 by 64^3 matrix. ToF-based methods mainly focus on efficient and robust algorithms to recover $\mathbf{x}$.

Recently, a forward model beyond a linear model has been studied. For example, the shape of the surface can be recovered using fewer photons by modeling photons that travel specific paths called Fermat paths [25]. Phasor-field virtual wave optics enables the modeling of full light transport, including photons that bounce more than three times, in the hidden scene [29].

Back-Projection: A naive way to solve Eq. 3 is to consider each voxel (an element in $\mathbf{x}$), and compute the heat map of an object occupying the voxel given the measurement $\mathbf{y}$ and light transport model $\mathbf{A}$. This back-projection method was exploited in the first demonstration of the 3D reconstruction of hidden objects [7], and other NLOS imaging works for reconstruction [14, 15, 17–20]. Back-projection usually produces blurry reconstruction, as shown in Fig. 6 (b) because of the ill-posed nature of $\mathbf{A}$. Sharpening filters and thresholding are used to improve the reconstruction quality. Instead of considering each voxel,

a probability map of $\mathbf{x}$ can be recovered by considering the intersections of ellipsoidal constraints to perform efficient back-projection that is up to three orders of magnitude faster than naive back-projection [16]. Back-projection can be implemented optically, by illuminating and scanning along ellipsoids on the relay wall. This enables focusing the measurement to a single voxel in the hidden scene [23].

Optimization: Priors on the hidden object $\mathbf{x}$ can be incorporated to the inversion of Eq. 3 by formulating the inverse problem as minimization of a least square error with a regularizer [13, 14, 21, 27, 28]:

$$\hat{\mathbf{x}} = \arg \min_x \|\mathbf{y} - \mathbf{A}\mathbf{x}\|^2 + \Gamma(\mathbf{x}), \qquad (4)$$

where $\Gamma(\mathbf{x})$ encourages $\mathbf{x}$ to follow priors of the hidden scene. Iterative algorithms such as CoSaMP [76], FISTA [77], and ADMM [78] can be used to solve this optimization problem based on the priors. Enforcing priors generally results in better reconstruction quality as compared to back-projection.

While computation and memory complexity can be enormous, the optimization formulation gives flexibility in more accurate reconstruction. For example, $\mathbf{A}$ can be factorized to consider partial occlusion and surface normal of the hidden object to recover the visibility and surface normal as well as the albedo of the hidden object [13].

Confocal Imaging: In confocal imaging, the relay wall is raster-scanned as the detector collects photons from the same point as the illuminated spot [12]. This makes $w_1 = w_2$, and the ellipsoidal constraints become spherical constraints, which makes the forward operation a 3D convolution (Fig. 7). Confocal setup relaxes the need to solve back-projection or optimization

problems, and instead, a simple deconvolution solves the reconstruction problem. 3D deconvolution makes confocal imaging both memory- and computationally-efficient. Confocal imaging makes the inverse problem simple but suffers from the first-bounce photons as the detection and illumination points are the same. This issue can be mitigated by introducing a slight misalignment of the detector and illumination or time gating of SPAD. However, SNR is still limited because the single-bounce light is much stronger than the three-bounce light.

The above three methods formulate NLOS imaging as a linear inverse problem. Other problem formulations can be constructed to solve NLOS imaging from different perspectives.

Wave-Based reconstruction: Reza et al. [79] showed that the intensity waves from modulated light in the NLOS setting can be modeled as a propagation of a wave (phasor field). The hidden scene's impulse response can be recorded with a pulsed laser and ultrafast detector such as SPAD. The modulated light pulse can be virtually synthesized over time, using the recorded impulse response. Constructive interference of the synthesized wave appears at the hidden object. Hence, virtual propagation of a pulsed modulation on the impulse response of the hidden scene results in reconstruction [29]. Virtual wave optics approach to NLOS imaging models the full light transport, including more than three-bounce photons in the hidden scene. Lindel et al. [30] modeled the light transport of the confocal imaging system as wave propagation, where the measurement is one boundary condition. Acquiring other boundary conditions of the wave propagation with frequency-wavenumber (f-k) migration algorithm results in efficient and robust reconstruction of the hidden scene containing objects with various surface reflectance.

Inverse Rendering: A renderer can be used to model the physics-based forward model instead of analytical forward operations, as written in Eq. 3. This "synthesis-by-analysis" approach, also known as inverse rendering, changes the scene parameters such that the rendered and experimental measurements match. Inverse rendering provides more flexible reconstructions than the voxel-based reconstruction discussed above. For example, more detailed reconstruction is possible by representing the hidden object in mesh, and non-Lambertian surface reflection can be incorporated [22]. However, accurate rendering can be time-consuming, especially because each iteration of the optimization requires computationally expensive rendering. The long run-time problem can be solved by a differential renderer that efficiently computes gradients with respect to the hidden scene parameters [26].

Shape Recovery: Methods discussed above use full ToF measurement for reconstruction. However, the surface can be recovered without using all the multi-bounce photons. Tsai et al. showed that the first-returning photons provide the length of the shortest path to the hidden object, which can be used to reconstruct the boundary and surface normal of the hidden object [24]. Later, discontinuities of ToF measurement are shown to follow specific paths (Fermat paths) that give rich information about the boundary of the hidden geometry [25]. Because this approach does not rely on intensity information, it is robust to BRDF variations of the object around corners.

2.2. Inference Algorithms for Localization, Tracking, and Classification

We have reviewed algorithms to reconstruct objects around the corners. Often, reconstruction of the hidden object might not be the end goal. Instead, the inference of the properties of the hidden object, such as its location or class is sufficient. While reconstruction suffices such tasks, direct inference without reconstruction can be made more efficiently with a smaller number of measurements.

Back-Projection: The back-projection algorithm that we discussed in the reconstruction section can be used for a point localization. Instead of considering small voxels to recover the details of the object, an object can be treated as the single voxel to recover the location of the object [42, 43]. Because the goal is not to recover the 3D shape, localization can be performed with much fewer measurements and less computation than reconstruction at a larger scale [43]. While reconstruction of the cluttered scene is challenging, tracking and size estimation of a moving object is demonstrated by Pandharka et al. [41].

Deep learning: Data-driven algorithms have become a powerful tool for pattern recognition and found promising applications in computer vision. Though data-driven approaches for full reconstruction require further theoretical development [80, 81], deep learning is useful for inference of unknown parameters such as object class and location. The objective of deep learning approach is to learn $x = f^{-1}(y)$, where $f(\cdot)$ could be hard to model explicitly. For example, neural networks with a SPAD array demonstrated the point localization and identification of a person around the corner [45]. While the imaging setup is different from a corner, Satat et al. [82] demonstrated calibration-free NLOS classification of objects behind a diffuser, where
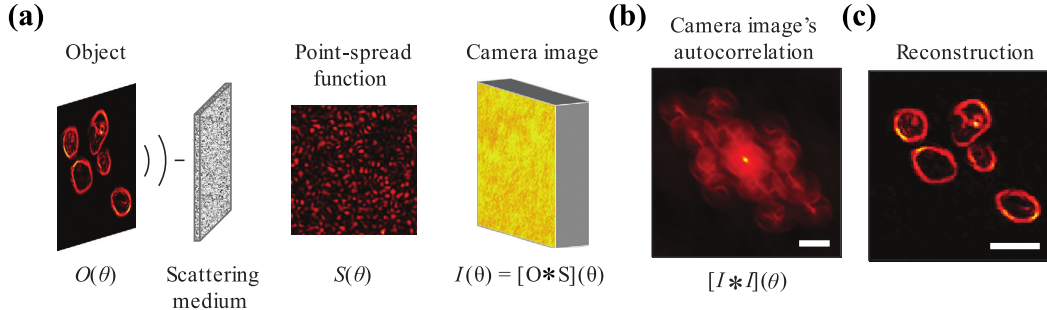
Figure 8: **The principle of speckle-based imaging technique to image after diffuse scattering (Material from: Katz et al., "Non-invasive single-shot imaging through scattering layers and around corners via speckle correlations," published 2014, Nature Photonics [8], adapted with permission of SNCSC).** (a) Camera captures speckle pattern after scattering on a diffuse wall. (b) The angular auto-correlation of the captured image is the same as the angular auto-correlation of the original image. (c) Phase-retrieval algorithms recover the image before the scattering on the wall.

the transmissive scattering at the diffuser is similar to the reflective scattering at the relay wall.

3. Coherence-based NLOS Imaging

The challenges of NLOS imaging come from the scattering of photons on the diffuse relay wall. However, some coherent properties of light are preserved after scattering. Coherence-based methods exploit speckle patterns or spatial coherence to see around corners.

3.1. Speckle-Based NLOS Imaging:

The speckle pattern is an intensity fluctuation generated by the interference of the coherent light waves. Although a speckle pattern may seem random, the observed pattern encodes information about the hidden scene.

Reconstruction The angular correlation of the object intensity pattern is preserved in the observed speckle pattern after the scattering on the relay wall [83]. This is known as memory effect [84, 85]:

$$\mathbf{y} * \mathbf{y} = \mathbf{x} * \mathbf{x}, \tag{5}$$

where $\mathbf{y}$ and $\mathbf{x}$ are the observed speckle pattern and object intensity pattern, respectively. $*$ denotes convolution. Katz et al. [8] found that the memory effect can be applied to a spatially incoherent light source such as fluorescent bulb, and demonstrated single-shot imaging through scattering, and around corners. Reconstruction of the hidden object can be performed with phase-retrieval algorithms [86, 87]. Speckle pattern can also be generated with active coherent illumination when the speckle pattern cannot be observed in passive sensing [32]. While this approach achieves

diffraction-limited resolution, its field of view is limited because of the memory effect(order of a few degrees of the angular field of view [8]). Because scattering of the diffuse wall has a similar nature as the scattering of a diffuser, speckle-based reconstruction can be used to see through scattering media as well [88].

Inference for Tracking When coherent light illuminates objects around a corner, the light scattered from the objects creates a speckle pattern on the relay wall. When the object moves, the speckle pattern moves as well. The motion of the object can be tracked by computing the cross-correlation of two images taken at different times [89]. Smith et al. [47] showed that this principle applies to NLOS imaging, and demonstrated motion tracking of the multiple hidden reflectors using the active coherent illumination. The speckle-based tracking has precision less than 10 μm, but is currently limited to microscopic motions because of the small field of view of the memory effect [47]. The data-driven approach demonstrated MNIST and pose-estimation classification from speckle patterns [51].

3.2. Spatial-Coherence-Based NLOS Imaging:

Spatial coherence refers to the correlation of the phase of a light wave at different observation points (while temporal coherence refers to the correlation at different observation time). Spatial coherence can be used to reconstruct the scene in the camera's field of view [90]. Because the spatial coherence of light is preserved through the scattering at the diffuse wall, such reconstruction techniques can be applied to NLOS imaging [33, 34]. Measurement of spatial coherence requires a unique imaging system such as the Dual-Phase Sagnac Interferometer (DuPSaI) [57].
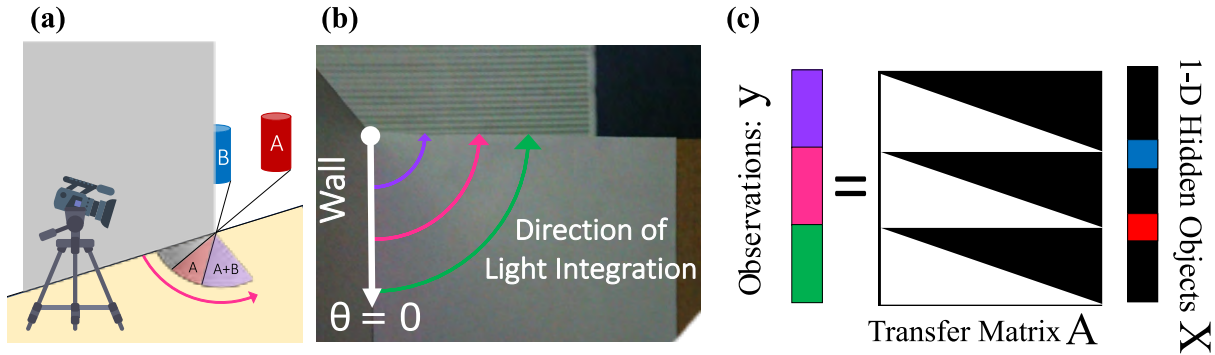
Figure 9: **The layout of NLOS imaging exploiting the scene occlusion (Material from: Bouman et al., "Turning Corners into Cameras: Principles and Methods," published 2017 [11] adapted with permission from IEEE. © 2017 IEEE).** (a) The corner occlusion casts shadows that depend on the location of the hidden objects. (b) Intensity camera sees the intensity over the angle from the relay wall. (c) Transfer (measurement) matrix **A** is constructed based on the occlusion.
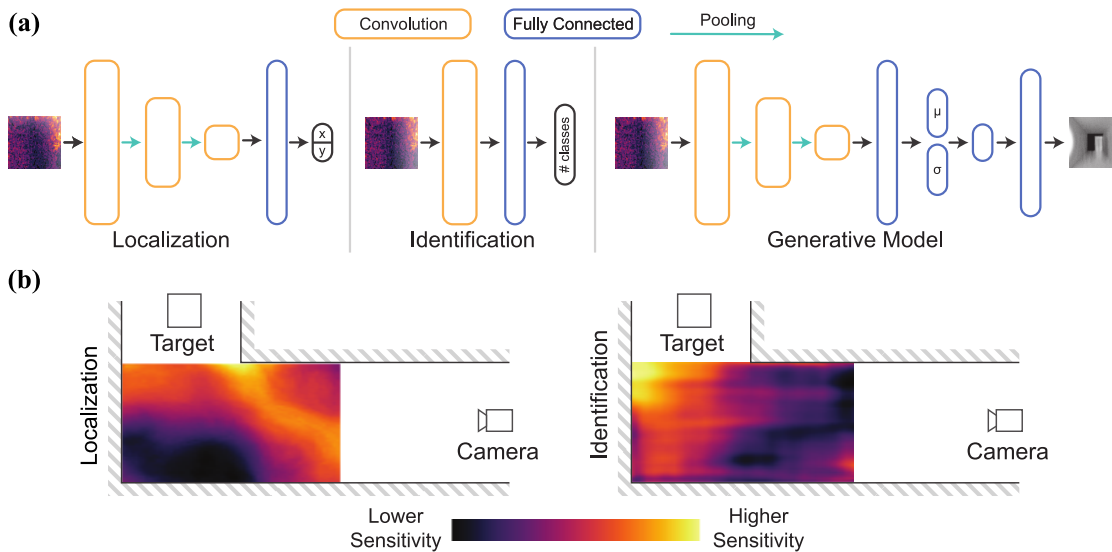

Figure 10: **Neural networks can locate, classify and reconstruct the hidden scene (Material from: Tancik et al., "Flash Photography for Data-Driven Hidden Scene Recovery," published 2018 [10] adapted with permission from the authors).** (a) Neural network architectures for different tasks. (b) Heatmaps of "important" region of the scene for localization and identification tasks. Neural networks learn to exploit the occlusion as proposed by [11] (left). It also learns to use measurements that are previously not realized to be useful for object identification tasks (right).

Reconstruction The propagation of coherence in free space can be approximated in a closed-form. This lets the spatial coherence measurement **y** be expressed as a system of linear equations as written in Eq. 3, where **A** illustrates the propagation of the spatial coherence function through space and scattering. This inverse problem can be solved as minimization of least square error and regularizers that incorporate priors such as sparsity and small total variation. Beckus et

al. [34] showed that coherence measurement and intensity measurement could be incorporated into a single optimization problem for reconstruction.

Inference for Localization Using spatial coherence, the distance of the incoherent light source from the detector can be estimated from the phase of the spatial coherence function. While only 1D localization was demonstrated [33], multiple measurements of the spatial coherence functions can be used to localize the

light source by triangulation.

4. Intensity-Based NLOS Imaging

Velten et al. [7] first studied the use of intensity measurement for NLOS imaging and showed that a traditional camera requires high sensitivity for diffuse surfaces. We illustrate this in Fig. 4, and refer readers to the supplemental material of [7] for further details. To overcome this challenge, most of the existing intensity-based NLOS imaging works exploit occlusions in the scene. Before the development of NLOS imaging, occlusions have been used for computational imaging for a long time. For example, light transport from occlusions are used to synthesize images from a different point of view [91], spatially varying BRDF to capture incident light [92], recover 4D light field for refocusing [93], and create an anti-pinhole camera to see outside the field-of-view of the camera [94]. Tancik et al. [9, 10] and Bouman et al. [11] first addressed the NLOS imaging problem directly. Bouman et al. showed 1D tracking, and Tancik et al. introduced the idea of using intensity-based reconstruction for NLOS imaging. We also review another class of technique that exploits non-Lambertian surface reflection.

4.1. Exploiting Occlusions

Spatially varying occlusions make it feasible to use intensity measurement since the variability of intensity due to occlusions increases the rank of the underlying ray transport matrix. Passive intensity-based NLOS imaging with inexpensive cameras has shown a real-time demonstration of seeing around corners. However, the separation of the ambient light and the signal light from the object is necessary, which often requires moving hidden objects or background subtraction.

Localization: Bouman et al. [11] demonstrated practical passive tracking of hidden objects using an occlusion from a wall as illustrated in Fig. 9(a), and Tankic et al. showed that neural networks learn to exploit occlusions [10] as shown in Fig. 10 (b) . The occlusion in the scene can be considered to be a specific type of aperture. As shown in Fig. 9 (c), the problem can be formulated as a linear inverse problem similar to Eq. 3, where $\mathbf{A}$ represents light transport with occlusions. With priors on the floor albedo, it is possible to estimate the 1D angular location the hidden object from a single measurement by estimating the ambient illumination [48].

Reconstruction: More complex occlusion geometries enable reconstruction of the hidden scene, as $\mathbf{A}$ becomes well-posed [38, 39]. A 4D light field can be recovered from an occlusion-based inverse problem

framework [37]. While the above reconstruction techniques assume known occlusions, the unknown occlusions can be estimated by exploiting the sparse motion of the hidden object [40]. Deep learning-based approaches showed its ability for reconstruction, tracking, and object classification to a specific scene setup, while its generalizability is yet to be explored [9,10,50].

4.2. Exploiting Surface Reflectance

Another class of intensity-based NLOS imaging technique exploits the bidirectional reflectance distribution function (BRDF) of the relay wall to reconstruct the hidden scene. Specular BRDF makes the inverse problem less ill-posed. When such reflectance function of the wall is known, the light field from the hidden scene can be reconstructed [36]. However, current demonstrations are limited to scenes without ambient light, and the wall has some specular surface reflections [36]. Chen et al. [31] demonstrated the reconstruction of specular planar objects with active illumination. The data-driven approach showed that it is also possible to reconstruct diffuse objects with active illumination [31]. Tracking of the object using active illumination and intensity measurement can be performed by matching the simulation with the experimental measurements (inverse rendering) [49]. Thermal imaging benefits from the specular BRDF of long-wave IR, which was exploited for passive localization and near real-time pose detection around corners [35].

5. Challenges and Future Directions

We reviewed major techniques for NLOS imaging in the previous sections. Here, we introduce common challenges to real-time and robust applications to inspire further research.

5.1. Properties of Different Sensing Modalities

Table 1 shows the current landscape of NLOS techniques, and Table 2 summarizes the properties of different sensing modalities. In this section, we discuss what challenges need to be solved to complete Table 1.

ToF: Since ToF-based NLOS imaging was first demonstrated, there have been significant improvements in reconstruction algorithms that became orders of magnitude faster than the originally proposed algorithm. The challenges towards practical ToF-based NLOS imaging are:

- Low signal-to-background of three-bounce photons.

- Estimation of line-of-sight scene parameters.

	Illumination	Sensor	Cost	Sensitivity to Ambient Light	Need of Priors on Geometry
Pulsed ToF	Pulsed Laser	Streak Camera SPAD	High	Robust	Not Required
AMCW ToF	Modulated Laser, LED	Correlation Camera	Medium	Sensitive to Strong Light	Not Required
Passive Coherence	None	Traditional Camera	Low	Sensitive	Scene Geometry
Passive Spatial Coherence	None	Dual Phase Sagnac Interferometer	Medium	Sensitive	Scene Geometry
Active Coherence	Coherent Source	Traditional Camera	Low	Sensitive	Scene Geometry
Passive Intensity	None	Traditional Camera	Low	Sensitive	Scene Geometry Occlusion Geometry
Active Intensity	Flashlight Laser	Traditional Camera	Low	Sensitive	Scene Geometry

Table 2: **Properties of techniques to see around corner for different sensing schemes.** This table summarizes fundamental properties of seeing around corners techniques.

First, only a small fraction of the emitted photons are captured in the measurement. This limits the acquisition time for NLOS imaging. Many recent works still require minutes to an hour of acquisition time for diffuse objects, which limits the real-time applications. Second, the majority of the existing works treat the line-of-sight scene as a known geometry, given that the line-of-sight scene is much easier to recover than the hidden scene. However, a fully-automated procedure to recover both line-of-sight and non-line-of-sight geometry is necessary for the practical applications of NLOS imaging, where the imaging platform could be moving.

Coherence: The coherence-based approaches exploit the observations that certain coherent properties are preserved after the scattering on the diffuse wall. The challenge towards practical speckle-based methods are:

- Small field-of-view due to memory effect.

- Lack of depth information.

Correlography techniques exploit memory effect, which has a limited angular field of view [8]. This limits its application to the macroscopic scenes such as autonomous vehicles. Speckle-based reconstruction methods recover the 2D projection of the image but do not recover the depth.

Spatial coherence-based methods do not suffer from the small field of view as the speckle-based methods, but they require sensitive interferometric detectors that are mechanically translated [33].

Intensity: The ease of image acquisition is the main advantage of intensity-based approaches. Detection of hidden moving objects around corners using shadow was demonstrated on an autonomous wheelchair [95]. The challenge towards practical intensity-base NLOS imaging are:

- Unknown occluding geometries in the hidden scene.

- Separation of the background and signal photons.

- Low signal-to-noise ratio.

First, the quality of passive, occlusion-based NLOS imaging heavily depends on the occluding geometries. For example, if there are no occluding geometries in the hidden scene, the reconstruction is extremely challenging [38, 39]. However, such information about occlusions might not be available in prior. Second, ambient illumination may be much stronger than the signal light, which makes it hard to isolate the signal from the measurement. This requires active illumination, background subtraction, or motion of the hidden scene to extract the signal. Lastly, the algorithm has to be sensitive enough to capture the small signal from the hidden scene while robust enough to reject the intensity variation due to the noise.

5.2. Limitations on Reconstruction:

ToF-based NLOS imaging has a derived resolution limit. Reza et al. [79] showed that virtual optics formulation of NLOS imaging gives the following Rayleigh

lateral resolution limit:

$$\Delta x \approx 1.22 \frac{c\tau L}{d}, \qquad (6)$$

where c, τ, L, d are the speed of light, full-width-half-max of the temporal response of the imaging system, the distance between the wall and hidden object, and diameter of the virtual aperture (scanning area) respectively. However, it is hard to evaluate resolution for some NLOS imaging techniques. The reconstruction capability of occlusion-based techniques heavily relies on scene geometry. It is essential to evaluate different methods with common datasets such as those proposed in [96].

Liu et al. [97] showed that the hidden object becomes impossible to reconstruct depending on the direction of its surface normal. It is also shown that the reconstruction of multiple objects may fail with a simple linear light transport model when the signal from one object is stronger than the others [13]. Further theoretical investigation of such limitations is necessary for the practical use of NLOS imaging.

5.3. Acquisition Time

The low signal-to-noise ratio (SNR) or signal-to-background ratio is a common issue for most NLOS imaging techniques, as discussed in the previous section. This is a fundamental problem, as the number of photons from the hidden object is typically small. This limits the possible acquisition time necessary for satisfactory reconstruction and inference. Fig. 11 summarizes reported demonstration of NLOS imaging techniques across different scales of the acquisition time, illumination power, and scene.

Active Sensing: Most of the emitted photons will not be captured by the camera. Moreover, the 3-bounce photons that contain the information about the hidden scene consist only of a small fraction of the captured photons. Current demonstrations of real-time NLOS imaging with eye-safe power level is limited to retroreflective objects. Recent work on ToF-based NLOS imaging uses a laser of up to 1W power, but yet requires 10 minutes of acquisition time [30]. More than 10W power is necessary to perform reconstruction under a minute with the same quality, but increasing laser power is not scalable for safety and cost. One could use light at a different wavelength, such as near-infrared radiation, with higher eye safety power. Recently, a new scanning method was proposed to focus on a single voxel on the hidden scene, which can improve the SNR for a specific region of interest [23].

Passive Sensing: In many practical scenarios, most of the passively captured photons are ambient
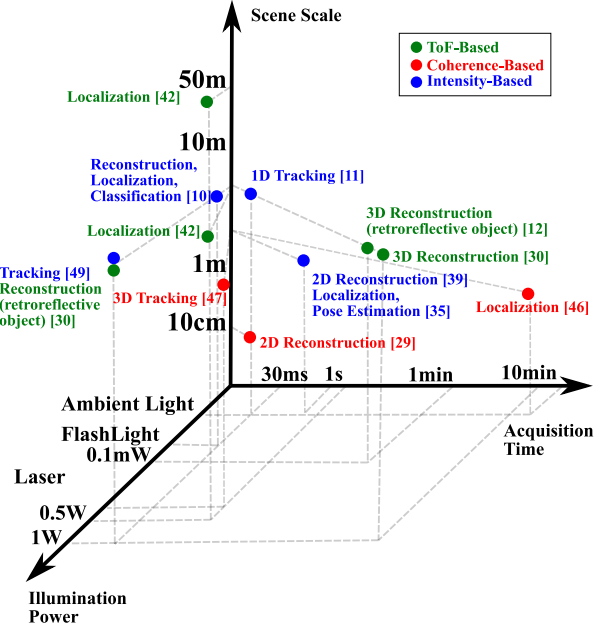

Figure 11: **Overview of the state-of-art NLOS imaging demonstration across different acquisition time, illumination power, and scene scale.**

light, which does not interact with the hidden objects. This results in low SNR as well as the necessity to separate ambient photons and photons from the hidden objects. The signal photons can be isolated by exploiting the movements in the hidden scene [11], or background subtraction when a measurement without the hidden object is available. Priors on the ambient illumination can also be exploited to remove the ambient term from the measurement [48]. Because uncontrolled ambient light is hard to model, adding an active illumination to the passive technique may improve the signal to noise ratio [10, 50].

5.4. Integration of Multi-Modal Techniques

The measurements from different sensing modalities can be jointly exploited for NLOS imaging. Becks et al. [34] showed that fused intensity measurement and coherence measurement in a single optimization framework produces better reconstruction results.

Insights from different approaches can be shared. For example, occlusions are not exploited in the ToF-based approaches. Occlusion-based techniques might be able to narrow down the region of interest in the hidden scene to make the ToF-based reconstruction faster.

5.5. Data-driven Approach

We refer "data-driven" approach to the use of data to model the mapping between the measurement and

the hidden scenes, and to produce priors on the solution to the inverse problem.

Learned Priors: Handcrafted priors such as total-variation are often used for NLOS reconstruction. More flexible priors or representations of the hidden objects can be learned from relevant data. Recent results on deep learning show the use of a generative model or discriminative model to enforce the learned priors in linear inverse problem [98, 99]. Theoretical connections between convolutional neural networks and dictionary learning [100] suggest the suitability of emerging deep learning methodology to incorporate learned representations as priors to solve inverse problems.

End-to-End Learning: In recent years, deep learning has demonstrated a powerful set of techniques with applications to pattern recognition and studied for computational imaging applications such as CT and MRI [101]. If there are correlations present in a dataset, then deep learning can offer powerful and flexible ways to approximate the function that maps the desired outputs from novel inputs. With a large dataset, a deep learning model can learn the mapping between a measurement and the desired inference (e.g., reconstruction and localization). The same network may also easily be adapted to learn the forward model as well by swapping the inputs and outputs and making changes to the model architecture. Potentially, a data-driven approach could offer calibration-free, efficient, and flexible solutions to NLOS imaging problems [9, 10, 31]. Fig. 10 shows the use of deep learning for localization, identification, and reconstruction around corners.

Many NLOS imaging methods attempt to find efficient and robust algorithms to solve the optimization problem shown in Eq. 3. In contrast, the data driven approach attempts to solve the following minimization problem to find the function $\hat{f}$, which approximates the mapping between the measurement y, and the target x (3D shape, location, class of the hidden object):

$$\hat{f} = \arg\min_{f \in \mathcal{F}} \frac{1}{n} \sum_{i=1}^{n} l(f(y_i), x_i) + r(\theta), \qquad (7)$$

where f is parameterized by θ and the regularizer $r(\theta)$ discourages over-fitting. $\frac{1}{n} \sum_{i=1}^{n} l(f(y_i), x_i)$ denotes the error between the reconstruction and ground truth.

The main problems in the data-driven approach are generalizability and explainability.

Generalizability: The potential advantage of data-driven approaches is that they can learn models that are more robust to scene variation than brittle model-based approaches. For example, a data-driven approach may handle variations in a wall reflectance, while a model-based approach is often limited to simple, diffuse reflectance. However, the key concern is data-driven approaches fail in unpredictable ways when encountering scenes that are not represented in the training data.

One approach towards generalization is to produce a sufficiently large dataset that contains rich variations such that any possible practical scenes are represented in the training dataset. However, this is ultimately limited by the ability to simulate or collect enough experimental data to sufficiently sample the parameter space. Another approach is to design flexible neural networks for specific scene types. This makes it easier for the neural networks to learn the algorithm, which robustly works if the scene type is identified correctly.

Explainability: Another challenge for data-driven approaches is that Eq. 7 produces a mapping that is difficult to interpret. Rather than incorporating a known forward model, the learned mapping is based on the statistics present in the training set and is susceptible to "hallucinating" output in order to produce a "reasonable output" with respect to the training data.

Instead of learning Eq. 7 directly, a combination of physics-based forward models and data-driven approaches could make these methods more explainable [102]. To solve the optimization problem in Eq. 3, iterative algorithms such as ADMM and ISTA demonstrate improved performance when learning priors or forward models from a specific distribution [80, 103, 104]. While traditional model-based approaches typically rely on a handcrafted sparsity prior, a data-driven approach could offer a prior that more accurately models the scene distribution [99, 100]. Furthermore, these algorithms can be embedded within the architecture of the deep learning model directly [105]. Incorporating data-driven techniques into the traditional model-based optimization schemes show promise for NLOS imaging without sacrificing explainability.

6. Conclusions and Future Directions

We reviewed the existing NLOS imaging techniques that rely on different principles and discussed challenges towards the practical, real-time NLOS imaging. We hope that this paper will help and inspire further research toward practical NLOS imaging.

7. Acknowledgement

References

[1] http://web.media.mit.edu/~raskar/cornar/.

[2] Fadel Adib and Dina Katabi. See through walls with wifi! *SIGCOMM Comput. Commun. Rev.*, 43(4):75–86, August 2013.

[3] Fadel Adib, Chen-Yu Hsu, Hongzi Mao, Dina Katabi, and Frédo Durand. Capturing the human figure through a wall. *ACM Trans. Graph.*, 34(6):219:1–219:13, October 2015.

[4] David B. Lindell, Gordon Wetzstein, and Vladlen Koltun. Acoustic non-line-of-sight imaging. In *IEEE Intl. Conf. Computer Vision and Pattern Recognition (CVPR)*, 2019.

[5] Ramesh Raskar and James Davis. 5 d time-light transport matrix : What can we reason about scene properties? 2008.

[6] Ahmed Kirmani, Tyler Hutchison, James Davis, and Ramesh Raskar. Looking around the corner using transient imaging. In *2009 IEEE 12th International Conference on Computer Vision*, pages 159–166, Sep. 2009.

[7] Andreas Velten, Thomas Willwacher, Otkrist Gupta, Ashok Veeraraghavan, Moungi G Bawendi, and Ramesh Raskar. Recovering three-dimensional shape around a corner using ultrafast time-of-flight imaging. *Nature communications*, 3:745, 2012.

[8] Ori Katz, Pierre Heidmann, Mathias Fink, and Sylvain Gigan. Non-invasive real-time imaging through scattering layers and around corners via speckle correlations. *Nature Photonics*, 8, 03 2014.

[9] Matthew Tancik, Tristan Swedish, Guy Satat, and Ramesh Raskar. Data-driven non-line-of-sight imaging with a traditional camera. In *Imaging and Applied Optics 2018 (COSI)*, page IW2B.6. Optical Society of America, 2018.

[10] Matthew Tancik, Guy Satat, and Ramesh Raskar. Flash photography for data-driven hidden scene recovery, 2018.

[11] Katherine L. Bouman, Vickie Ye, Adam B. Yedidia, Fredo Durand, Gregory W. Wornell, Antonio Torralba, and William T. Freeman. Turning corners into cameras: Principles and methods. In *2017 IEEE International Conference on Computer Vision (ICCV)*, pages 2289–2297, Oct 2017.

[12] Matthew O'Toole, David B. Lindell, and Gordon Wetzstein. Confocal Non-Line-of-Sight Imaging Based on the Light-Cone Transform. *Nature*, 2018.

[13] Felix Heide, Matthew O'Toole, Kai Zang, David B. Lindell, Steven Diamond, and Gordon Wetzstein. Non-line-of-sight imaging with partial occluders and surface normals. *ACM Trans. Graph.*, 2019.

[14] Otkrist Gupta, Thomas Willwacher, Andreas Velten, Ashok Veeraraghavan, and Ramesh Raskar. Reconstruction of hidden 3d shapes using diffuse reflections. *Opt. Express*, 20(17):19096–19108, Aug 2012.

[15] Mauro Buttafava, Jessica Zeman, Alberto Tosi, Kevin Eliceiri, and Andreas Velten. Non-line-of-sight imaging using a time-gated single photon avalanche diode. *Opt. Express*, 23(16):20997–21011, Aug 2015.

[16] Victor Arellano, Diego Gutierrez, and Adrian Jarabo. Fast back-projection for non-line of sight reconstruction. *Opt. Express*, 25(10):11574–11583, May 2017.

[17] Andreas Velten Martin Laurenzis. Nonline-of-sight laser gated viewing of scattered photons. *Optical Engineering*, 53:53 – 53 – 7, 2014.

[18] Marco La Manna, Fiona Kine, Eric Breitbach, J. Jackson, Talha Sultan, and Andreas Velten. Error backprojection algorithms for non-line-of-sight imaging. *IEEE transactions on pattern analysis and machine intelligence*, 2018.

[19] Martin Laurenzis, Jonathan Klein, Emmanuel Bacher, and Nicolas Metzger. Multiple-return single-photon counting of light in flight and sensing of non-line-of-sight objects at shortwave infrared wavelengths. *Opt. Lett.*, 40(20):4815–4818, Oct 2015.

[20] Chenfei Jin, Jiaheng Xie, Siqi Zhang, ZiJing Zhang, and Yuan Zhao. Reconstruction of multiple non-line-of-sight objects using back projection based on ellipsoid mode decomposition. *Opt. Express*, 26(16):20089–20101, Aug 2018.

[21] Adithya Pediredla, Mauro Buttafava, Alberto Tosi, Oliver Cossairt, and Ashok Veeraraghavan. Reconstructing rooms using photon echoes: A plane based model and reconstruction algorithm for looking around the corner. In *2017 IEEE International Conference on Computational Photography (ICCP)*, pages 1–12, May 2017.

[22] Julian Iseringhausen and Matthias B. Hullin. Non-line-of-sight reconstruction using efficient transient rendering, 2018.

[23] Adithya Pediredla, Akshat Dave, and Ashok Veeraraghavan. Snlos: Non-line-of-sight scanning through temporal focusing. 2019.

[24] Chia-Yin Tsai, Kiriakos Kutulakos, Srinivasa G. Narasimhan, and Aswin Sankaranarayanan. The geometry of first-returning photons for non-line-of-sight imaging. pages 2336–2344, 07 2017.

[25] Shumian Xin, Sotiris Nousias, Kiriakos N. Kutulakos, Aswin C. Sankaranarayanan, Srinivasa G. Narasimhan, and Ioannis Gkioulekas. A theory of fermat paths for non-line-of-sight shape reconstruction. In *Proceedings of the 2019 IEEE Conference on Computer Vision and Pattern Recognition*, CVPR '19. IEEE Computer Society, 2019.

[26] Chia-Yin Tsai, Aswin C. Sankaranarayanan, and Ioannis Gkioulekas. Beyond volumetric albedo — A surface optimization framework for non-line-of-sight imaging. In *IEEE Intl. Conf. Computer Vision and Pattern Recognition (CVPR)*, 2019.

[27] Felix Heide, Lei Xiao, Wolfgang Heidrich, and Matthias B. Hullin. Diffuse mirrors: 3d reconstruction from diffuse indirect illumination using inexpensive time-of-flight sensors. In *Proceedings of the 2014 IEEE Conference on Computer Vision and Pattern Recognition*, CVPR '14, pages 3222–3229, Washington, DC, USA, 2014. IEEE Computer Society.

[28] Achuta Kadambi, Hang Zhao, Boxin Shi, and Ramesh Raskar. Occluded imaging with time-of-flight sensors. *ACM Trans. Graph.*, 35:15:1–15:12, 2016.

[29] Xiaochun Liu, Ibón Guillén, Marco La Manna, Ji Hyun Nam, Syed Azer Reza, Toan Huu Le, Adrian Jarabo, Diego Gutierrez, and Andreas Velten. Non-line-of-sight imaging using phasor-field virtual wave optics. *Nature*, pages 1–4, 2019.

[30] David B. Lindell, Gordon Wetzstein, and Matthew O'Toole. Wave-based non-line-of-sight imaging using fast f-k migration. *ACM Trans. Graph. (SIGGRAPH)*, 38(4):116, 2019.

[31] Wenzheng Chen, Simon Daneau, Fahim Mannan, and Felix Heide. Steady-state non-line-of-sight imaging. In *The IEEE Conference on Computer Vision and Pattern Recognition (CVPR)*, June 2019.

[32] Aparna Viswanath, Prasanna Rangarajan, Duncan MacFarlane, and Marc P Christensen. Indirect imaging using correlography. In *Imaging and Applied Optics 2018 (3D, AO, AIO, COSI, DH, IS, LACSEA, LS&C, MATH, pcAOP)*, page CM2E.3. Optical Society of America, 2018.

[33] Mahed Batarseh, Sergey Sukhov, Zhean Shen, H Gemar, R Rezvani, and A Dogariu. Passive sensing around the corner using spatial coherence. *Nature Communications*, 9, 12 2018.

[34] Andre Beckus, Alexandru Tamasan, and George K. Atia. Multi-modal non-line-of-sight passive imaging. *IEEE Transactions on Image Processing*, 28(7):3372–3382, Jul 2019.

[35] Tomohiro Maeda, Yiqin Wang, Ramesh Raskar, and Achuta Kadambi. Thermal non-line-of-sight imaging. In *IEEE International Conference on Computational Photography(ICCP)*, 2019.

[36] Takahiro Sasaki and James R. Leger. Light-field reconstruction from scattered light using plenoptic data. *Proc. SPIE*, 10772:10772 – 10772 – 7, 2018.

[37] Manel Baradad, Vickie Ye, Adam B. Yedidia, Frédo Durand, William T. Freeman, Gregory W. Wornell, and Antonio Torralba. Inferring light fields from shadows. In *CVPR*, 2018.

[38] Christos Thrampoulidis, Gal Shulkind, Feihu Xu, William T. Freeman, Jeffrey H. Shapiro, Antonio Torralba, Franco N. C. Wong, and Gregory W. Wornell. Exploiting occlusion in non-line-of-sight active imaging. *IEEE Transactions on Computational Imaging*, 4:419–431, 2018.

[39] Charles Saunders, John Murray-Bruce, and Vivek Goyal. Computational periscopy with an ordinary digital camera. *Nature*, 565:472, 01 2019.

[40] Adam B. Yedidia, Manel Baradad, Christos Thrampoulidis, William T. Freeman, and Gregory W. Wornell. Using unknown occluders to

recover hidden scenes. In *The IEEE Conference on Computer Vision and Pattern Recognition (CVPR)*, June 2019.

[41] Rohit Pandharkar, Andreas Velten, Andrew Bardagjy, Everett Lawson, Moungi Bawendi, and Ramesh Raskar. Estimating motion and size of moving non-line-of-sight objects in cluttered environments. In *CVPR 2011*, pages 265–272, June 2011.

[42] Genevieve Gariepy, Francesco Tonolini, Ryan Warburton, Susan Chan, Robert Henderson, Jonathan Leach, and Daniele Faccio. Detection and tracking of moving objects hidden from view. In *Imaging and Applied Optics 2016*, page CTh4B.3. Optical Society of America, 2016.

[43] Susan Chan, Ryan E. Warburton, Geneviève Gariépy, Yoann Altmann, Stephen McLaughlin, Jonathan Leach, and Daniele Franco Angelo Faccio. Fast tracking of hidden objects with single-pixel detectors. *Electronics Letters*, 53(15):1005–1008, 7 2017.

[44] Susan Chan, Ryan E. Warburton, Genevieve Gariepy, Jonathan Leach, and Daniele Faccio. Non-line-of-sight tracking of people at long range. *Optics express*, 25 9:10109–10117, 2017.

[45] Piergiorgio Caramazza, Alessandro Boccolini, Daniel Buschek, Matthias B. Hullin, Catherine F. Higham, Robert Henderson, Roderick Murray-Smith, and Daniele Faccio. Neural network identification of people hidden from view with a single-pixel, single-photon detector. In *Scientific Reports*, 2018.

[46] Jeremy Boger-Lombard and Ori Katz. Non line-of-sight localization by passive optical time-of-flight. 08 2018.

[47] Brandon M. Smith, Matthew O'Toole, and Mohit Gupta. Tracking multiple objects outside the line of sight using speckle imaging. In *The IEEE Conference on Computer Vision and Pattern Recognition (CVPR)*, June 2018.

[48] Sheila W Seidel, Yanting Ma, John Murray-Bruce, Charles Saunders, Bill Freeman, Christopher Yu, and Goyal Vivek. Corner occluder computational periscopy: Estimating a hidden scene from a single photograph. 2019.

[49] Jonathan Klein, Christoph Peters, Jaime Martín, Martin Laurenzis, and Matthias B. Hullin.

Tracking objects outside the line of sight using 2d intensity images. *Scientific Reports*, 6(32491), August 2016.

[50] Sreenithy Chandran and Suren Jayasuriya. Adaptive lighting for data-driven non-line-of-sight 3d localization and object identification, May 2019.

[51] Xin Lei, Liangyu He, Yixuan Tan, Ken Xingze Wang, Xinggang Wang, Yihan Du, Shanhui Fan, and Zongfu Yu. Direct object recognition without line-of-sight using optical coherence. In *The IEEE Conference on Computer Vision and Pattern Recognition (CVPR)*, June 2019.

[52] Gao Liang, Liang Jinyang, Li Chiye, and V Wang Lihong. Single-shot compressed ultrafast photography at one hundred billion frames per second. *Nature*, 516:74–7, 2014.

[53] Bernhard Büttgen, Thierry Oggier, Michael Lehmann, Rolf Kaufmann, and Felix Lustenberger. Ccd / cmos lock-in pixel for range imaging : Challenges , limitations and state-ofthe-art. 2005.

[54] Buttgen Bernhard and Seitz Pater. Robust optical time-of-flight range imaging based on smart pixel structures. *IEEE Transactions on Circuits and Systems I: Regular Papers*, 55(6):1512–1525, July 2008.

[55] Lin Yang, Longyu Zhang, Haiwei Dong, Abdulhameed Alelaiwi, and Abdulmotaleb El Saddik. Evaluating and improving the depth accuracy of kinect for windows v2. *IEEE Sensors Journal*, 15:1–1, 08 2015.

[56] Florian Willomitzer, Fengqiang Li, Prasanna Rangarajan, and Oliver Cossairt. Non-line-of-sight imaging using superheterodyne interferometry. In *Imaging and Applied Optics 2018 (3D, AO, AIO, COSI, DH, IS, LACSEA, LS&C, MATH, pcAOP)*, page CM2E.1. Optical Society of America, 2018.

[57] Roxana Rezvani Naraghi, Heath Gemar, Mahed Batarseh, Andre Beckus, George Atia, Sergey Sukhov, and Aristide Dogariu. Wide-field interferometric measurement of a nonstationary complex coherence function. *Opt. Lett.*, 42(23):4929–4932, Dec 2017.

[58] Nikhil Naik, Shuang Zhao, Andreas Velten, Ramesh Raskar, and Kavita Bala. Single view

reflectance capture using multiplexed scattering and time-of-flight imaging. In *Proceedings of the 2011 SIGGRAPH Asia Conference*, SA '11, pages 171:1–171:10, New York, NY, USA, 2011. ACM.

[59] Guy Satat, Barmak Heshmat, Christopher Barsi, Dan Raviv, Ou Chen, Moungi G Bawendi, and Ramesh Raskar. Locating and classifying fluorescent tags behind turbid layers using time-resolved inversion. *Nature communications*, 6:6796, 04 2015.

[60] Anand T. N. Kumar, Scott Raymond, Greg Boverman, David Boas, and Brian J Bacskai. Time resolved fluorescence tomography of turbid media based on lifetime contrast. *Optics express*, 14:12255–70, 01 2007.

[61] Dan Raviv, Christopher Barsi, Nikhil Naik, Micha Feigin, and Ramesh Raskar. Pose estimation using time-resolved inversion of diffuse light. *Opt. Express*, 22(17):20164–20176, Aug 2014.

[62] Guy Satat, Barmak Heshmat, Dan Raviv, and Ramesh Raskar. All photons imaging through volumetric scattering. *Scientific Reports*, 6:33946, 09 2016.

[63] Guy Satat, Matthew Tancik, and Ramesh Raskar. Towards photography through realistic fog. In *2018 IEEE International Conference on Computational Photography (ICCP)*, pages 1–10, May 2018.

[64] Andreas Velten, Di Wu, Adrián Jarabo, Belén Masiá, Christopher Barsi, Chinmaya Joshi, Everett Lawson, Moungi Bawendi, Diego Gutierrez, and Ramesh Raskar. Femto-photography: capturing and visualizing the propagation of light. *ACM Trans. Graph.*, 32:44:1–44:8, 2013.

[65] Achuta Kadambi, Refael Whyte, Ayush Bhandari, Lee Streeter, Christopher Barsi, Adrian Dorrington, and Ramesh Raskar. Coded time of flight cameras: Sparse deconvolution to address multipath interference and recover time profiles. *ACM Trans. Graph.*, 32(6):167:1–167:10, November 2013.

[66] Ayush Bhandari, Achuta Kadambi, Refael Whyte, Christopher Barsi, Micha Feigin, Adrian Dorrington, and Ramesh Raskar. Resolving multipath interference in time-of-flight imaging via modulation frequency diversity and sparse regularization. *Opt. Lett.*, 39(6):1705–1708, Mar 2014.

[67] Achuta Kadambi, Ayush Bhandari, Refael Whyte, Adrian Dorrington, and Ramesh Raskar. Demultiplexing illumination via low cost sensing and nanosecond coding. pages 1–10, 05 2014.

[68] Di Wu, Andreas Velten, Matthew O'Toole, Belen Masia, Amit Agrawal, Qionghai Dai, and Ramesh Raskar. Decomposing global light transport using time of flight imaging. *International Journal of Computer Vision*, 107(2):123–138, Apr 2014.

[69] Genevieve Gariepy, Nikola Krstajic, Robert K. Henderson, Chunyong Li, Robert R. Thomson, Gerald S. Buller, Barmak Heshmat, Ramesh Raskar, Jonathan Leach, and Daniele Faccio. Single-photon sensitive light-in-fight imaging. In *Nature communications*, 2015.

[70] Achuta Kadambi, Jamie Schiel, and Raskar Raskar. Macroscopic interferometry: Rethinking depth estimation with frequency-domain time-of-flight. In *2016 IEEE Conference on Computer Vision and Pattern Recognition (CVPR)*, pages 893–902, June 2016.

[71] M. O'Toole, F. Heide, D. Lindell, K. Zang, S. Diamond, and G. Wetzstein. Reconstructing Transient Images from Single-Photon Sensors. *Proc. IEEE CVPR*, 2017.

[72] Guy Satat, Matthew Tancik, and Ramesh Raskar. Lensless imaging with compressive ultrafast sensing. *IEEE Transactions on Computational Imaging*, PP, 10 2016.

[73] Barmak Heshmat, Ik Hyun Lee, and Ramesh Raskar. Optical brush: Imaging through permuted probes. *Scientific Reports*, 6:20217, 02 2016.

[74] Barmak Heshmat, Matthew Tancik, Guy Satat, and Ramesh Raskar. Photography optics in the time dimension. *Nature Photonics*, 12, 09 2018.

[75] Steven M. Seitz, Yasuyuki Matsushita, and Kiriakos N. Kutulakos. A theory of inverse light transport. In *Proceedings of the Tenth IEEE International Conference on Computer Vision - Volume 2*, ICCV '05, pages 1440–1447, Washington, DC, USA, 2005. IEEE Computer Society.

[76] Deanna Needell and Joel A. Tropp. Cosamp: Iterative signal recovery from incomplete and inaccurate samples. *Communications of the ACM*, 53, 12 2010.

[77] Amir Beck and Marc Teboulle. Fast gradient-based algorithms for constrained total variation image denoising and deblurring problems. *IEEE Transactions on Image Processing*, 18(11):2419–2434, Nov 2009.

[78] Stephen Boyd, Neal Parikh, Eric Chu, Borja Peleato, and Jonathan Eckstein. Distributed optimization and statistical learning via the alternating direction method of multipliers. *Found. Trends Mach. Learn.*, 3(1):1–122, January 2011.

[79] Syed Azer Reza, Marco La Manna, and Andreas Velten. A physical light transport model for non-line-of-sight imaging applications. *arXiv preprint arXiv:1802.01823*, 2018.

[80] Karol Gregor and Yann LeCun. Learning fast approximations of sparse coding. In *ICML*, 2010.

[81] Xiaohan Chen, Jialin Liu, Zhangyang Wang, and Wotao Yin. Theoretical linear convergence of unfolded ista and its practical weights and thresholds. In S. Bengio, H. Wallach, H. Larochelle, K. Grauman, N. Cesa-Bianchi, and R. Garnett, editors, *Advances in Neural Information Processing Systems 31*, pages 9079–9089. Curran Associates, Inc., 2018.

[82] Guy Satat, Matthew Tancik, Otkrist Gupta, Barmak Heshmat, and Ramesh Raskar. Object classification through scattering media with deep learning on time resolved measurement. *Opt. Express*, 25(15):17466–17479, Jul 2017.

[83] Isaac Freund. Looking through walls and around corners. *Physica A-statistical Mechanics and Its Applications - PHYSICA A*, 168:49–65, 09 1990.

[84] Shechao Feng, Charles Kane, Patrick A. Lee, and A.Douglas Stone. Correlations and fluctuations of coherent wave transmission through disordered media. *Physical review letters*, 61:834–837, 09 1988.

[85] Isaac Freund, M Rosenbluh, and Shechao Feng. Memory effects in propagation of optical waves through disordered media. *Physical review letters*, 61:2328–2331, 12 1988.

[86] Yoav Shechtman, Yonina C. Eldar, Oren Cohen, Henry N. Chapman, Jianwei Miao, and Mordechai Segev. Phase retrieval with application to optical imaging, 2014.

[87] Kishore Jaganathan, Yonina C. Eldar, and Babak Hassibi. Phase retrieval: An overview of recent developments, 2015.

[88] Jacopo Bertolotti, Elbert G. van Putten, Christian Blum, Ad Lagendijk, W. Vos, and Allard P. Mosk. Non-invasive imaging through opaque scattering layers. *Nature*, 491:232–234, 2012.

[89] Brandon M. Smith, Pratham Desai, Vishal Agarwal, and Mohit Gupta. Colux: Multi-object 3d micro-motion analysis using speckle imaging. *ACM Trans. Graph.*, 36(4):34:1–34:12, July 2017.

[90] Andre Beckus, Alexandru Tamasan, Aristide Dogariu, Ayman F. Abouraddy, and George K. Atia. On the inverse problem of source reconstruction from coherence measurements. *J. Opt. Soc. Am. A*, 35(6):959–968, Jun 2018.

[91] Pradeep Sen, Billy Chen, Gaurav Garg, Stephen R. Marschner, Mark Horowitz, Marc Levoy, and Hendrik P. A. Lensch. Dual photography. In *ACM SIGGRAPH 2005 Papers*, SIGGRAPH '05, pages 745–755, New York, NY, USA, 2005. ACM.

[92] Neil G. Alldrin and David J. Kriegman. A planar light probe. In *Proceedings of the 2006 IEEE Computer Society Conference on Computer Vision and Pattern Recognition - Volume 2*, CVPR '06, pages 2324–2330, Washington, DC, USA, 2006. IEEE Computer Society.

[93] Ashok Veeraraghavan, Ramesh Raskar, Amit Agrawal, Ankit Mohan, and Jack Tumblin. Dappled photography: Mask enhanced cameras for heterodyned light fields and coded aperture refocusing. In *ACM SIGGRAPH 2007 Papers*, SIGGRAPH '07, New York, NY, USA, 2007. ACM.

[94] Antonio Torralba and William T. Freeman. Accidental pinhole and pinspeck cameras: Revealing the scene outside the picture. In *2012 IEEE Conference on Computer Vision and Pattern Recognition*, pages 374–381, June 2012.

[95] Felix Naser, Igor Gilitschenski, Guy Rosman, Alexander Amini, Fredo Durand, Antonio Torralba, Gregory W. Wornell, William T. Freeman, Sertac Karaman, and Daniela Rus. Shadowcam: Real-time detection of moving obstacles behind a corner for autonomous vehicles. pages 560–567, 11 2018.

[96] Jonathan Klein, Martin Laurenzis, Dominik Ludewig Michels, and Matthias B. Hullin. A quantitative platform for non-line-of-sight imaging problems. In *BMVC*, 2018.

[97] Xiaochun Liu, Sebastian Bauer, and Andreas Velten. Analysis of feature visibility in non-line-of-sight measurements. In *The IEEE Conference on Computer Vision and Pattern Recognition (CVPR)*, June 2019.

[98] Ashish Bora, Ajil Jalal, Eric Price, and Alexandros G. Dimakis. Compressed sensing using generative models. In Doina Precup and Yee Whye Teh, editors, *Proceedings of the 34th International Conference on Machine Learning*, volume 70 of *Proceedings of Machine Learning Research*, pages 537–546, International Convention Centre, Sydney, Australia, 06–11 Aug 2017. PMLR.

[99] Sebastian Lunz, Carola Schoenlieb, and Ozan Öktem. Adversarial regularizers in inverse problems. In S. Bengio, H. Wallach, H. Larochelle, K. Grauman, N. Cesa-Bianchi, and R. Garnett, editors, *Advances in Neural Information Processing Systems 31*, pages 8516–8525. Curran Associates, Inc., 2018.

[100] Aviad Aberdam, Jeremias Sulam, and Michael Elad. Multi-layer sparse coding: The holistic way. *SIAM Journal on Mathematics of Data Science*, 1(1):46–77, 2019.

[101] Kyong Hwan Jin, Michael Mccann, Emmanuel Froustey, and Michael Unser. Deep convolutional neural network for inverse problems in imaging. *IEEE Transactions on Image Processing*, 26(9):4509–4522, Sep. 2017.

[102] Chengqian Che, Fujun Luan, Shuang Zhao, Kavita Bala, and Ioannis Gkioulekas. Inverse transport networks, 2018.

[103] Yan Yang, Jian Sun, Huibin Li, and Zongben Xu. Deep admm-net for compressive sensing mri. In D. D. Lee, M. Sugiyama, U. V. Luxburg, I. Guyon, and R. Garnett, editors, *Advances in Neural Information Processing Systems 29*, pages 10–18. Curran Associates, Inc., 2016.

[104] J H. Rick Chang, Chun-Liang Li, Barnabas Poczos, B Kumar, and Aswin Sankaranarayanan. One network to solve them all — solving linear inverse problems using deep projection models. In *2017 IEEE International Conference on Computer Vision (ICCV)*, pages 5889–5898, Oct 2017.

[105] Steven Diamond, Vincent Sitzmann, Felix Heide, and Gordon Wetzstein. Unrolled optimization with deep priors, 2017.